IEEE Access
Multidisciplinary | Rapid Review | Open Access Journal

Received December 3, 2019, accepted December 31, 2019, date of publication January 13, 2020, date of current version January 17, 2020.

Digital Object Identifier 10.1109/ACCESS.2020.2965216

Passive Measurement Method of Tree Height and Crown Diameter Using a Smartphone

WU XINMEI, XU AIJUN, AND YANG TINGTING

School of Information Engineering, Zhejiang Agriculture Forestry University, Hangzhou 311300, China
Key Laboratory of State Forestry and Grassland Administration on Forestry Sensing Technology and Intelligent Equipment, Zhejiang Agriculture Forestry University, Hangzhou 311300, China
Zhejiang Provincial Key Laboratory of Forestry Intelligent Monitoring and Information Technology, Zhejiang Agriculture Forestry University, Hangzhou 311300, China

Corresponding author: Xu Aijun (xuaj1976@zafu.edu.cn)

This work was supported in part by the China National Natural Science Foundation 31670641, in part by the Zhejiang Science and Technology Key Research and Development Program 201018C02013,and in part by the Key Laboratory of State Forestry and Grassland Administration on Forestry Sensing Technology and Intelligent Equipment, and in part by the Zhejiang Provincial Key Laboratory of Forestry Intelligent Monitoring and Information Technology for Smartphone and Field Equipment.

ABSTRACT The tree height and crown diameter are important measurement attributes in forest resource survey and management. Hence, we propose a passive measurement method of tree height and crown diameter based on monocular camera of a smartphone. First, we use an feature-adaptive Mean-Shift algorithm to segment the image and extract tree's contour. Furthermore, an adaptive feature coordinate system is established to help study the conversion relationship of the coordinate systems. It has been proved that for the image points with the same abscissa pixels, their ordinate pixels have a linear relationship with its actual imaging angles. A depth extraction model is built according to this principle. Then, we obtain the rotation and translation matrix and established tree height and crown diameter models according to the mapping transformation relationship of coordinates. Experimental results reveal significant correlation between calculated and truth values. The RMSE is 0.267 m (rRMS=2.482%) for tree height and 0.209 m (rRMS=5.631%) for crown diameter. The relative errors of tree heights are less than 5.76% (MRE=2.159%); for crown diameter, the relative errors are less than 9.73% (MRE=4.95%). Overall, the accuracy of this method falls within the requirements of the continuous inventory of Chinese national forest resources.

INDEX TERMS Tree height, crown diameter, monocular vision, passive Measurement, depth extraction model.

I. INTRODUCTION

As important tree attributes in forest survey and management, the tree height and crown diameter, can be used to evaluate the site's productive capacity and tree's growth status [1]–[3]. The measurement of tree attributes also have biological and commercial values [4]. They can be used to estimated biomass, green space and so on. Traditional tree height and crown diameter measurement instruments, such as angle gauge, total station and so on, are expensive, time or labor consuming [5], [6]. Additionally, the tree attributes can also be estimated according to the allometric relationship of crown diameter, diameter at breast height, and height [7], [8]. However, to build this kind of allometric relationship, we need a large amount of dataset, and the accuracy of these methods might be compromised by insufficient data and possible violation of tree growth [9]. It is significant to develop scientific and emerging technologies to measure tree attributes [10], and explore means to minimize resource requirements, e.g., cost, labor, time etc. [11].

With the development of remote sensor and machine vision, non-contact measurement methods have emerged, and the measurement methods of tree attributes are gradually developing towards smart, high precision and efficiency [12], [13]. Non-contact measurement methods are mainly divided into active and passive ranging methods. These methods provide efficient way to estimate tree height and crown diameter [14], [15]. The remote sensing technology supports for large-scale forest resource survey and management, which can help to timely understand the

The associate editor coordinating the review of this manuscript and approving it for publication was Md. Moinul Hossain.

dynamic changes of vegetation [16]. Compared with optical remote sensing technology, 3D lidar has higher measurement accuracy and faster data processing speed [17], [18]. Ferraz, A. et al. [19] apply a statistical approach based on the Mean-Shift algorithm to decompose the ALS point cloud into 3D segments corresponding to individual vegetation features. The algorithm is robust enough for characterizing multi-layered forests. However, for general forestry survey enthusiasts who are not expert in this field these active measurement instruments are limited. It requires expert knowledge, which limits its' use in daily practice [20], [21]. Structured-light measurement is also a kind of passive ranging method which is effective in measuring the 3D geometry size of industrial work-pieces, depth extracting and so on. But it is not robust enough in nature environment, because the coded spot emitted by the laser is easily flooded by sunlight. Ultrasound technology calculates the distance and extracts DBH based on acoustic wave propagation and time differences. Unfortunately, due to its long-range measurement system using ultrasonic range sensor with high-power transmitter and cumbersome instruments, the ultrasonic methods are difficult to be carried carried in field measurements [22], [23].

Machine vision, including both monocular and binocular vision [24]–[26], is a kind of passive optical technology, which estimates object size from image information. It has the advantages of rich image information and low cost [27]–[29]. The early image information extraction methods are mostly based on the binocular stereo vision or camera motion, and required multiple images [30]–[32]. In contrast, monocular methods do not require strict hardware conditions and are convenient for device integration [33]. Using a monocular vision system to measure tree attributes from image firstly requires to extract tree depth. Camera calibration can be used to study the conversion relationship between the image and the world coordinate system [34]–[36]. For large-scale scene, this method requires calibration checkerboard images in different orientations, and need to record the corresponding coordinate of each point in the world coordinate system and image coordinate system. Xiaodong and Zhongke [37] use digital camera to obtain two pictures in the up-down direction of the sample plot. The measured length of one object in the image is used to calculate the photographic baseline. Then the diameters of the sample trees are measured by calculating the real-space ratio relationship. However, this method requires more than one pictures, and the length of one object in the image need to be measured in advance. Additionally, due to the integration of various sensors in smartphone, many scholars have developed some tree attributes measurement platforms based on smartphone. By placing a calibrator in the scenes and calculating its ratio, Zhou Keyu *et al.* [38] use the trigonometric principle to measure tree height. To measure the trunk height and DBH, Guan Fangli [39] extract the trunk and calibrated the smartphone, 3D world coordinate pixel is then reconstructed using camera parameters and 2D image information. Overall, most of the passive measurement methods based on monocular vision are for single tree, and different forms of calibration board or multiple images are required to derive tree attributes. However, a compact design and user-friendly application using the portable smartphone can bring the measurement method based on monocular vision into wider range of users.

The aim of this study is to propose a passive measurement method for multi-tree heights and crown diameters based on monocular vision. Its key contribution was to measure trees attributes using smartphones, which is convenient, efficient and with high accuracy. We present tree height model (THM) and crown diameter model (CDM), and calculate tree attributes from the image. We then assess the accuracy of height and crown diameter measurements derived from models compared with their true values.

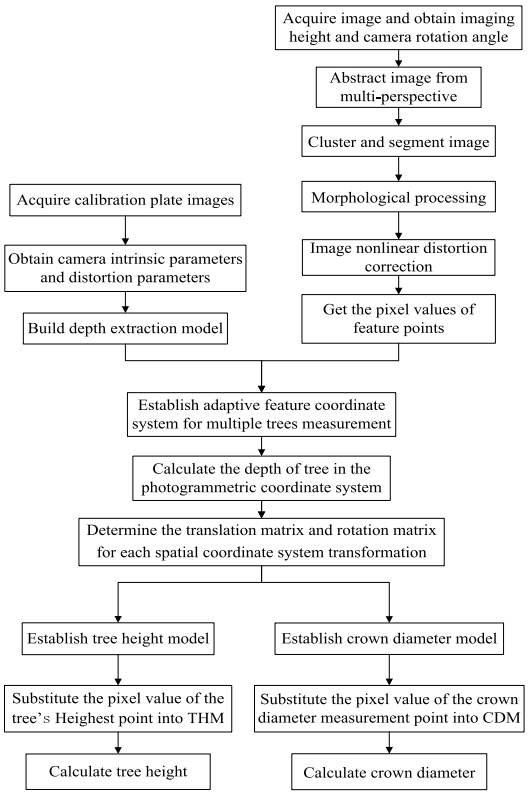

FIGURE 1. General framework of multiple trees' measurement method.

II. MATERIALS AND METHODS

A. ANALYSIS OVERVIEW

An illustration of our approach is described in Figure 1. Image is acquired through the smartphone with monocular vision camera. Then, we cluster and segment the image to obtain tree's contour. To increase the measurement accuracy, we correct the image using the nonlinear corrected model of camera. Furthermore, we establish an adaptive feature coordinate system and build a depth extraction model which is suitable for different models of smartphones. In addition, based on the conversion principle between coordinate systems, the THM and CDM are established respectively to calculate the tree height and crown diameter.

B. STUDY AREA AND IMAGE ACQUISITION

This study is carried out in an unmanaged forest in HangZhou city, north of Zhejiang province, in southeast coast of China (119.72E, 30.23N). And the forest cover rate attains 76.55%. Our study area is located on a terrain with moderate slope, and trees are heterogeneous, multi-aged mixed species. More than 3000 species of vegetation in the area.

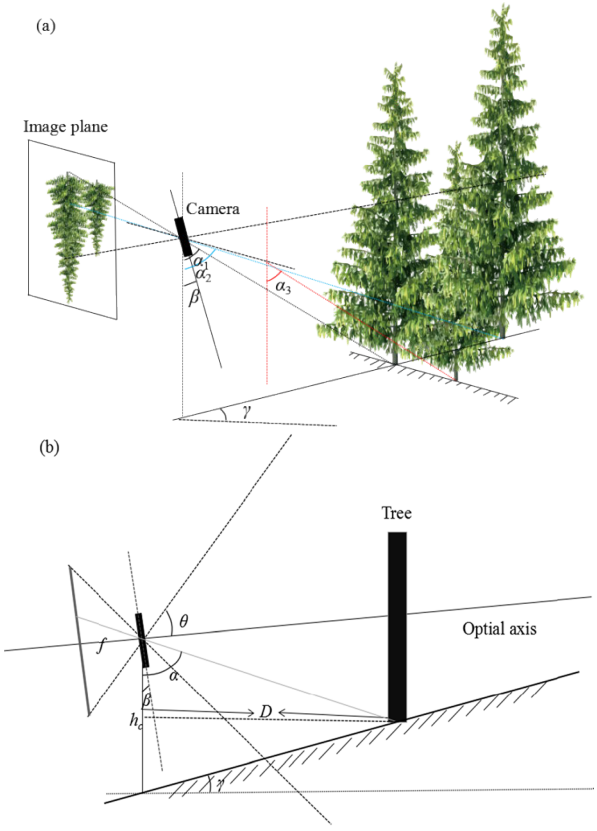

FIGURE 2. Stereo (a) and plane (b) projection geometry model of image.

Figure 2 describes the projection geometry model of image (Figure 2a is the stereo projection geometry model of image and Figure 2b is the plane projection geometry model of image). In these figures, f denotes the focal length of the camera, θ denotes half of the camera angle of view, h_c is the height of the camera. These parameters can be obtained through measurement or camera calibration. The camera rotation angle β (positive β values represent clockwise rotation) can be derived from the gravity sensor embed in the smartphone. α is the actual imaging angle of a target tree. D represents the depth of tree. γ denotes the slope of the ground.

C. CONTOUR EXTRACTION OF TREE

We segment and extract the tree's contour to obtain the pixel coordinates of the feature points, e.g. the geometrical center point of the tree's bottom, the tree's highest point and the crown's widest points. Figure 3a is the original image of tree. The tree's image is segmented by a multi-dimensional feature adaptive Mean-Shift algorithm. The Mean-Shift algorithm is an effective non-linear filter that looks for local maxima

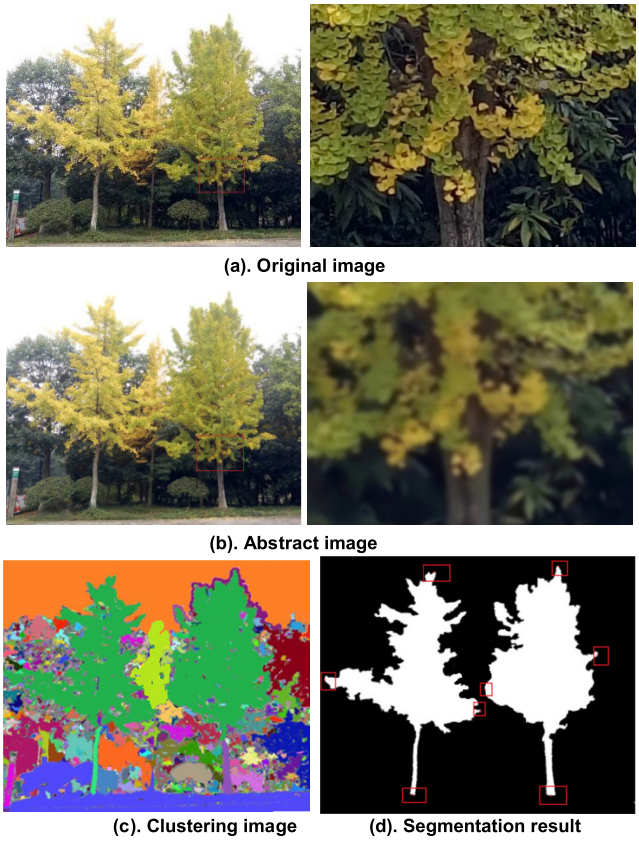

FIGURE 3. Extraction result of trunk contour.

(modes) of a density function [19]. It is a non-parametric and unsupervised approach, which only requires a single criterion (the kernel bandwidth) [40]. It has been widely used for image segmentation and other applications in recent years. Since there are too many noises in the background of the original image of tree collected in natural environment, such as soil, houses, roads, etc. And there are many small hollows and obvious texture details in branches and leaves in the canopy. So texture feature and noises can not be ignored when segments tree's image. A meaningful and reasonable image pre-processing is key for using the Mean-Shift algorithm to segment tree's image.

Three steps are contained in this algorithm: to obtain an abstract saliency map of the image, we blur and smooth the image by bilateral filtering and image pyramid processing; Combined the tree's features, such as spatial, color and texture, we then determine the bandwidth and kernel function parameters of the Mean-Shift algorithm and cluster image; Finally, the segmentation result is acquired by binaryzation and morphological expansion and erosion.

Image abstraction includes two parts: bilateral filtering and image pyramid processing. Smoothing the image by bilateral filtering can reduce the effects of complex backgrounds, trunks and foliage textures. Furthermore, the image pyramid method is used to further blur and smooth the image: the Gaussian kernel convolution is used to smooth and downsample the image, it can not only ensure the low-

pass filter of the tree's image, but also maintain the brightness of the image after shrinking and smoothing, thereby reducing the gap between the branches and leaves, and smoothing the crown texture. Then, the downsampled image is upsampled to restore the resolution size, and it can further abstract trees in the image. Finally, an abstract saliency map of the tree is obtained (Fig. 3b).

The image is clustered by Mean-Shift algorithm. The bandwidth of the iterative process has a great influence on the image segmentation quality, the convergence speed and accuracy of the algorithm. Thus, based on the features of trees, we select three types of feature vectors: spatial, color and texture to estimate the corresponding feature bandwidth. The spatial bandwidth h_s is related to the spatial coordinates of the pixel points, and it not only affects the mis-segmentation rate of the image, but also has influence on the running speed of the algorithm by iterations. In addition, the tree's image is transformed from RGB space to HSI color space. In this space, the visual saliency description of the tree in nature environment is introduced to make it one of the features of the recognition target, whereby I denotes luminance component which can effectively reduce the influence of illumination on image clustering. And then the adaptive color bandwidth h_r is obtained using the insertion rule method. What's more, texture features are added in the clustering process. And the gray level co-occurrence matrix method is used to calculate the texture bandwidth h_t through three common feature vectors, such as contrast ratio, energy and inverse moment, which improves the robustness of image clustering. After normalized the eigenvectors, the Gauss kernel function is used to perform Mean-Shift clustering. The kernel function is:

$$K_{h_s,h_r,h_t}(x) = \frac{D}{h_s^2 h_r^2 h_t^d} K(||\frac{x^s - x_i^s}{h_s}||^2) K(||\frac{x^r - x_i^r}{h_r}||^2) \times K(||\frac{x^t - x_i^t}{h_t}||^2) \quad (1)$$

where D denotes the normalization constant, and (x_i^s, x_i^r, x_i^t) are the spatial, color, and texture feature vectors of x adjacent to the sample point, respectively. Therefore, translation vector of the multidimensional feature adaptive Mean-Shift algorithm is:

$$m_{h_s h_r h_t}(x) = \frac{\sum_{i=1}^{n} x_i \exp(||\frac{x^s - x_i^s}{h_s}||^2) \exp(||\frac{x^r - x_i^r}{h_r}||^2) \exp(||\frac{x^t - x_i^t}{h_t}||^2)}{\sum_{i=1}^{n} \exp(||\frac{x^s - x_i^s}{h_s}||^2) \exp(||\frac{x^r - x_i^r}{h_r}||^2) \exp(||\frac{x^t - x_i^t}{h_t}||^2)} \quad (2)$$

A clustering image is shown in Fig. 3c.

After binarizing the clustering image, the segmentation result of the tree is acquired by morphological expansion, erosion repair. These steps can connect the adjacent objects to ensure the integrity of the target region and remove independent noise. Finally, the contour of the tree is obtained (Fig. 3d).

To adapt to the characteristics of the smartphone camera lens, calibration method proposed by Zhang Zhengyou [41], [42] with an improved nonlinear distortion term is used to calibrate the camera and obtain the camera intrinsic parameters and the nonlinear distortion parameters. We then use the nonlinear distortion parameters to correct distortion of the image.

D. MEASUREMENT METHODS OF TREE HEIGHT AND CROWN DIAMETER

We establish the coordinate system and build a depth extraction model. And then determine the intrinsic and extrinsic orientation elements of the camera and the conversion relationship between the spatial coordinate systems, which play an important role in establishing THM and CDM.

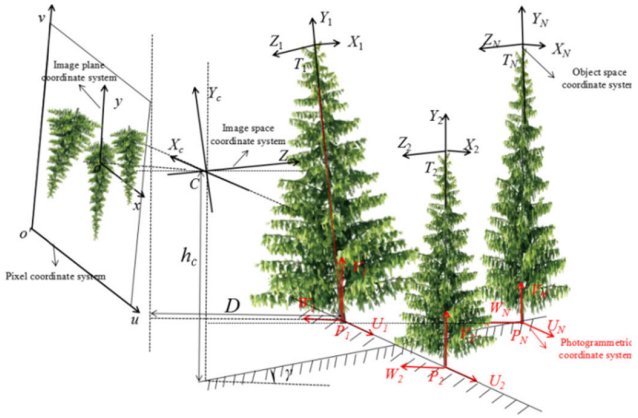

FIGURE 4. Adaptive feature coordinate system for multiple trees measurements.

1) COORDINATE SYSTEM ESTABLISHMENT

We establish an adaptive feature coordinate system (Figure 4). Particularly, It contains N sets of photogrammetric coordinate system and object space coordinate system for each tree to be measured in the image (N denotes the number of trees in the image). The origin of the photogrammetric coordinate system for the i-th tree D_i locates at the geometric center of the tree's bottom, the V_i axis is perpendicular to the horizontal surface, and the U_i axis is parallel to the image plane. The photogrammetric coordinate system translates h meter (h denote the tree height) along the main trunk and then rotates at a certain angle to obtain the object space coordinate system of that tree. The object space coordinate system Y_i axis lies vertically upward along the trunk.

2) TREE HEIGHT MODEL

According to the establishment rules of adaptive feature coordinate system, the object space coordinate system can be rotated and translated to the photogrammetric coordinate system. The origin of object space coordinate system $T_i - X_i Y_i Z_i$ can be expressed in the photogrammetric coordinate system $D_i - U_i V_i W_i$ as (U_{i0}, V_{i0}, W_{i0}):

$$\begin{bmatrix} U_{i0} & V_{i0} & W_{i0} \end{bmatrix}^{\mathrm{T}} = \boldsymbol{R}^i_{T-P} \cdot \boldsymbol{T}^i_{T-P} \quad (3)$$

whereby, translation matrix $\boldsymbol{T}^{i}_{T-P} = [0, h, 0]^{\mathrm{T}}$. The rotation relationship between the object space coordinate system and the photogrammetric coordinate system is defined as 0-φ-Ψ, with the Y_i axis as the principal axis. The system rotates φ degrees around the X_i axis, and rotates Ψ degrees around the new Z_i axis. Therefore, the rotation matrix $\boldsymbol{R}^{i}_{T-P}$ can be expressed as:

$$\boldsymbol{R}^{i}_{T-P} = \begin{bmatrix} \cos\psi & -\sin\psi & 0 \\ \cos\varphi\sin\psi & \cos\varphi\cos\psi & -\sin\varphi \\ \sin\varphi\sin\psi & \sin\varphi\cos\psi & \cos\varphi \end{bmatrix} \tag{4}$$

Combining the geometrical features of tree, φ and Ψ can be merged into the same angle, that is $\varphi = 0°$. The rotation angle Ψ can be obtained by extracting the minimum bounding rectangle of the trunk contour in the image. We then have:

$$\begin{aligned} \begin{bmatrix} U_{i0} \\ V_{i0} \\ W_{i0} \end{bmatrix} &= \begin{bmatrix} \cos\psi & -\sin\psi & 0 \\ \sin\psi & \cos\psi & 0 \\ 0 & 0 & 1 \end{bmatrix} \begin{bmatrix} 0 \\ h \\ 0 \end{bmatrix} \\ &= \begin{bmatrix} -h\sin\psi \\ h\cos\psi \\ 0 \end{bmatrix} \end{aligned} \tag{5}$$

The translation and rotation from the photogrammetric coordinate system to the image space coordinate system are two forms of rigid body motions. The photogrammetry coordinate system translates t_U, t_V and t_W distances (unit: mm) along the U_i, V_i and W_i axes. The rotation relationship between photogrammetry coordinate system and image space coordinate system is defined as κ-β-ω, with the V_i axis as the principal axis. For each object point in the i-th tree, its coordinates (X, Y, Z) in the image space coordinate system can be derived from (U_i, V_i, W_i), we then have:

$$\begin{bmatrix} X \\ Y \\ Z \end{bmatrix} = \boldsymbol{R} \begin{bmatrix} U_i \\ V_i \\ W_i \end{bmatrix} + \boldsymbol{T} = \boldsymbol{R} \left(\begin{bmatrix} U_i \\ V_i \\ W_i \end{bmatrix} + \begin{bmatrix} t_U \\ t_V \\ t_W \end{bmatrix} \right) \tag{6}$$

where $\boldsymbol{T}$ denotes the translation matrix from the photogrammetry coordinate system to the image space coordinate system, and $\boldsymbol{R}$ denotes the rotation matrix:

$$\begin{aligned} \boldsymbol{R} &= \begin{bmatrix} r_{11} & r_{12} & r_{13} \\ r_{21} & r_{22} & r_{23} \\ r_{31} & r_{32} & r_{33} \end{bmatrix} \\ r_{11} &= \cos\kappa\cos\omega - \sin\kappa\sin\beta\sin\omega \\ r_{12} &= -\cos\kappa\sin\omega - \sin\kappa\sin\beta\cos\omega \\ r_{13} &= -\sin\kappa\cos\beta \\ r_{21} &= \cos\beta\sin\omega \\ r_{22} &= \cos\beta\cos\omega \\ r_{23} &= -\sin\beta \\ r_{31} &= \sin\kappa\cos\omega + \cos\kappa\sin\beta\sin\omega \\ r_{32} &= -\sin\kappa\sin\omega + \cos\kappa\sin\beta\cos\omega \\ r_{33} &= \cos\kappa\cos\beta \end{aligned} \tag{7}$$

According to the establishment rules of the coordinate system, the rotation angle κ is 180°, and ω is approximately equal to 0°. This is because, when the image is collected, the smartphone is placed vertically on the camera tripod. $[t_U, t_V, t_W]^{\mathrm{T}}$ can be expressed as:

$$\begin{bmatrix} t_U \\ t_V \\ t_W \end{bmatrix} = \begin{bmatrix} t_U \\ -h_c + D\tan\gamma \\ -D \end{bmatrix} \tag{8}$$

We have the origin coordinate of the object space coordinate system in the image space coordinate system (X_0, Y_0, Z_0):

$$\begin{aligned} \begin{bmatrix} X_0 \\ Y_0 \\ Z_0 \end{bmatrix} = \boldsymbol{R} \begin{bmatrix} U_{i0} \\ V_{i0} \\ W_{i0} \end{bmatrix} + \boldsymbol{T} &= \begin{bmatrix} 1 & 0 & 0 \\ 0 & \cos\beta & -\sin\beta \\ 0 & -\sin\beta & -\cos\beta \end{bmatrix} \\ &\times \begin{bmatrix} -h\sin\psi + t_U \\ h\cos\psi - h_c + D\tan\gamma \\ -D \end{bmatrix} \end{aligned} \tag{9}$$

Therefore we have:

$$Z_0 = -(h\cos\psi - h_c + D\tan\gamma)\sin\beta + D\cos\beta \tag{10}$$

The Y value of the target tree's highest point can be expressed as:

$$Y_0 = (h\cos\psi - h_c + D\tan\gamma)\cos\beta + D\sin\beta \tag{11}$$

Let the physical size of each pixel on the image plane be $d_x * d_y$ (unit: mm) and the origin's coordinates of the image plane coordinate system in the pixel coordinate system be (u_0, v_0). Therefore, any image point satisfies the following relationship:

$$\begin{cases} u = x/d_x + u_0 \\ v = y/d_y + v_0 \end{cases} \tag{12}$$

where (x, y) denotes the coordinates of the image point in the image plane coordinate system, (u, v) denotes the coordinates of the image point in the pixel coordinate system. In the pinhole camera imaging model, the image point, the camera's optical center and the object point are collinear, and we have:

$$\begin{cases} x = f \cdot X/Z \\ y = f \cdot Y/Z \end{cases} \tag{13}$$

where (X, Y, Z) denotes the coordinates in the image space coordinate system. Let $a = y/f$, we derive:

$$a = Y/Z = (v - v_0)/f_y \tag{14}$$

Given camera intrinsic parameters, the tree height can be expressed as (15), as shown at the bottom of the next page, where a_0 is the ratio of the y coordinate of the tree's highest point in image plane coordinate system to the camera focal length.

Experiment showed that for the image points with the same abscissa pixels, their ordinate pixels have a linear relationship with the corresponding object points' actual imaging

angles [43]. According to this principle, we get the depth extraction model $F(\alpha, \beta)$:

$$F(v,\beta)=\begin{cases}\alpha=-\dfrac{\arctan\frac{v_{\max}}{2f_y}+\beta}{v_{\max}-v_0+\tan\beta\cdot f_y}v+90\\ +\dfrac{(v_0-\tan\beta\cdot f_y)\cdot(\arctan\frac{v_{\max}}{2f_y}+\beta)}{v_{\max}-v_0+\tan\beta\cdot f_y}\pm\delta & \theta>\beta\\ \alpha=-\dfrac{2\arctan\frac{v_{\max}}{2f_y}}{v_{\max}}v+90\\ +\arctan\dfrac{v_{\max}}{2f_y}-\beta\pm\delta & \theta<\beta\end{cases} \tag{16}$$

where δ denotes the nonlinear distortion parameter of the camera. Then, we can derived the depth of the tree:

$$D=\frac{h_c\cdot\tan\alpha}{1+\tan\gamma\cdot\tan\alpha} \tag{17}$$

3) CROWN DIAMETER MODEL

Due to the asymmetry of the crown, the CDM was constructed with the calculating of the crown widths on Z_i axis' left and right sides respectively to derive the crown diameter of tree.

In the adaptive feature coordinate system, the object space coordinate system of the i-th tree and it's photogrammetric coordinate system have the following relationship:

$$\begin{bmatrix}U_i\\V_i\\W_i\end{bmatrix}=\boldsymbol{R}^i_{T-P}\left(\begin{bmatrix}X_i\\Y_i\\Z_i\end{bmatrix}+\boldsymbol{T}^i_{T-P}\right) \tag{18}$$

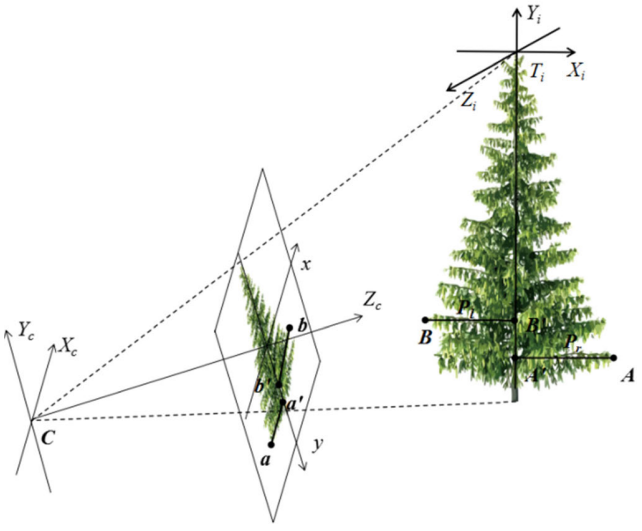

FIGURE 5. Projection geometry model of canopy measurement.

As shown in Figure 5, let the coordinates of the i-th tree's right crown measurement position be $A(X_i^A, Y_i^A, 0)$, then the coordinates of point A' are $(0, Y_i^A, 0)$. Points A and A' in the image space coordinate system are respectively projected to points $a(x_1, y_1)$ and $a'(x_2, y_2)$ in the image plane coordinate system. The coordinates of points a and a' in the pixel coordinate system are (u_1, v_1), (u_2, v_2), respectively. According to formula (18), the coordinates of point $A'(U_i^{A'}, V_i^{A'}, W_i^{A'})$ in the photogrammetric coordinate system can be derived:

$$\begin{aligned}\begin{bmatrix}U_i^{A'}\\V_i^{A'}\\W_i^{A'}\end{bmatrix}&=\begin{bmatrix}\cos\psi & -\sin\psi & 0\\ \sin\psi & \cos\psi & 0\\ 0 & 0 & 1\end{bmatrix}\begin{bmatrix}0\\Y_i^A+h\\0\end{bmatrix}\\&=\begin{bmatrix}-(Y_i^A+h)\sin\psi\\(Y_i^A+h)\cos\psi\\0\end{bmatrix}\end{aligned} \tag{19}$$

The coordinates $(X_{A'}, Y_{A'}, Z_{A'})$ of point A' can be calculated by combining formulas (6) and (19):

$$\begin{aligned}\begin{bmatrix}X_{A'}\\Y_{A'}\\Z_{A'}\end{bmatrix}&=\boldsymbol{R}\left(\begin{bmatrix}U_i^{A'}\\V_i^{A'}\\W_i^{A'}\end{bmatrix}+\boldsymbol{T}\right)=\begin{bmatrix}1 & 0 & 0\\0 & \cos\beta & -\sin\beta\\0 & -\sin\beta & -\cos\beta\end{bmatrix}\\&\times\begin{bmatrix}-(Y_i^A+h)\sin\psi+t_U\\(Y_i^A+h)\cos\psi-h_c+D\tan\gamma\\-D\end{bmatrix}\end{aligned} \tag{20}$$

We then have (21), as shown at the bottom of the next page, where $a_1=(v_1-v_0)/f_y$. Therefore, we have:

$$Z_A=Z_{A'}=-(\cos\psi(Y_i^A+h)-h_c+D\tan\gamma)\sin\beta+D\cos\beta \tag{22}$$

The horizontal parallax d of points A and A' is:

$$\begin{aligned}d&=x_2-x_1=f\cdot X_A/Z_A\\&=(u_2-u_1)\cdot d_x\end{aligned} \tag{23}$$

Hence, we get the right crown width P_r:

$$P_r=|X_A\cdot\cos\psi|=\frac{|u_2-u_1|\cdot Z_A}{f_x}\cdot\cos\psi \tag{24}$$

Similarly, the left crown width P_l can be calculated. Therefore, the crown diameter P can be expressed as:

$$P=P_l+P_r=\frac{(|u_2-u_1|\cdot Z_A)+(|u_4-u_3|\cdot Z_B)}{f_x}\cdot\cos\psi \tag{25}$$

where u_3 and u_4 are the abscissa pixel of the image points b and b', respectively, and Z_B is the coordinate of point B on the Z_c axis in the image space coordinate system.

E. STATISTICS AND VALIDATION OF DATA

To evaluate the accuracy of THM and CDM, we compare the calculated tree height and crown diameter with their truth values, we use linear regression analysis to model the relationship between the calculated and truth tree attributes (include tree height and crown diameter) and calculate the

$$h=\frac{(a_0\cdot D+h_c-D\tan\gamma)\cos\beta+(a_0\cdot h_c-D-\mathrm{a}_0\cdot D\tan\gamma)\sin\beta}{(a_0\sin\beta+\cos\beta)\cos\psi} \tag{15}$$

root mean square error (RMSE) and the coefficient of determination (R^2). Furthermore, the relative error root mean square (rRMS) is implemented to assess the deviation degree of the relative error. Additionally, box-and-whisker plots are used to illustrate the tree attributes. As a better illustration for the distribution of error, we also compute the mean absolute error (MAE) and mean relative error (MRE).

III. RESULTS

To verify the accuracy of THM and CDM, we use Xiaomi 3 (MI 3) smartphone to acquire images and verify the accuracy of tree height and crown diameter. The intrinsic parameters of MI 3 camera are $f_x = 3486.5637$, $u_0 = 569.0383$, $f_y = 3497.4652$, $v_0 = 2107.9899$, and the image resolution is 3120×4208.

We put the smartphone on camera tripod for image acquisition, and the camera height h_c is 1040 mm. 55 trees are measured by our method in this paper.

The tree heights and crown diameters measurement results are summarized in Figure 6(a) and (b) respectively. The relative errors of tree heights did not exceed 5.76% (MRE=2.159%). These errors fall within the accuracy requirements of Chinese national forest resources continuous inventory. Meanwhile, the relative errors of crown diameter are less than 9.734% (MRE=4.95%).

Linear regression analysis (Figure 6a) results show that the tree height measurement is highly correlated between calculated and truth values ($R^2 = 0.9874$, RMSE=0.267). Similarly, the crown diameter also exhibit a strong relationship between the calculated and truth values ($R^2 = 0.9614$, RMSE=0.209) (Figure 6b). We also calculate the absolute errors of tree height (Figure 7a) and crown diameter (Figure 7b). More specifically, the MAE of tree height measurement is 0.233 m and crown diameter measurement is 0.190 m. Furthermore, tree height measurements have an absolute errors between $-0.526 \sim 0.39$ m, and crown diameter measurements between -0.328 m and 0.322 m. Additionally, we also calculate the tree height rRMS = 2.482% and the crown diameter rRMS = 5.631%.

IV. DISCUSSION

The tree height and crown diameter are the significant tree's attributes in forest inventories. Crown height model and terrestrial measurement may be used to estimate tree attributes [44], [45]. Panagiotidis *et al.* [45] achieves tree height RMSE <3.08 m and crown diameter RMSE<1.04 m. For LIDAR, Kato Akira *et al.* [46] reports RMSE of tree height measurements of 1.56 m and 1.41 m and of crown diameter measurements of 0.93 m and 2.89 m respectively for coniferous and deciduous trees.

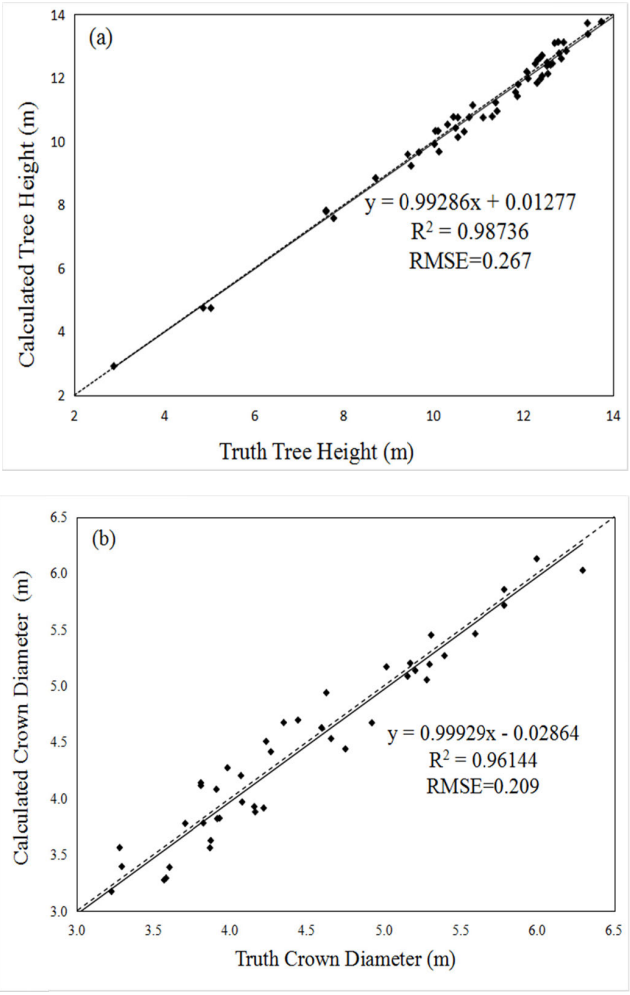

FIGURE 6. Linear regression model of the calculated and truth tree heights (a) and crown diameters (b).

In this study, we build the THM and CDM to derive the tree heights and crown diameters using smartphone. To validate the accuracy of the measurements results, the relationship between the truth and calculated values are tested. For both tree height and crown diameter, the calculated values have a strong relationship with the truth values (tree height RMSE=0.267 m, crown diameter RMSE=0.209 m)(Table 1). These results are consistent with most of the tree height and crown diameter measurement methods [45], [46]. But the overestimated and underestimated values are uniform distributed in our paper. And the RMSE values are relative lower. Calculated tree heights have an absolute errors between $-0.526 \sim 0.39$ m, MRE for tree height is 2.159% (rRMS=2.482%). For crown diameter, the absolute errors are between $-0.328 \sim 0.322$ m, while MRE is 4.95% (rRMS=5.631%), which is still acceptable when compared with other measurement methods [45], [47]–[49].

$$Y_i^A = \frac{(a_1 \cdot D + h_c - D\tan\gamma)\cos\beta + (a_1 \cdot h_c - D - \mathrm{a}_1 \cdot D\tan\gamma)\sin\beta}{(a_1\sin\beta + \cos\beta)\cos\psi} - h \tag{21}$$

TABLE 1. Statistical summary of tree height and crown diameter.

	Sample size	MAE /m	MRE /%	RMSE /m	rRMS /%
Tree height	55	0.233	2.159	0.267	2.482
Crown diameter	55	0.19	4.95	0.209	5.631

TABLE 2. Consistency test results of tree height and crown diameter.

Consistency test results of tree height and crown diameter	Paired Differences					t State	df	p-Value (2-tail)
	Mean (m)	Std. Bias (m)	Std. error mean (m)	95%Confidence interval of the difference				
				Upper	Lower			
Tree height	0.067	0.261	0.035	0.137	-0.004	1.902	54	0.063
Crown diameter	0.032	0.208	0.028	0.088	-0.025	1.123	54	0.266

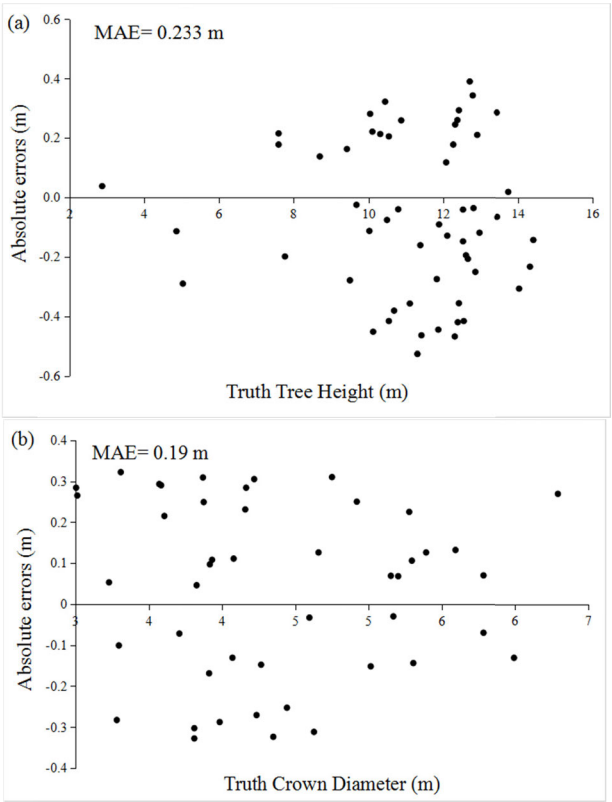

FIGURE 7. Absolute error distribution of the tree heights (a) and crown diameters (b).

We also use the t-test to verify the consistency of tree height and crown diameter. Experiment results show that null hypothesis are accepted, the difference of means between calculated tree height and truth tree height, and between calculated crown diameter and truth crown diameter are both non-significance according to two-tail t-test ($p > 0.05$) (Table 2). Meanwhile, the Std. bias of the tree height and crown diameter are 0.261 m and 0.208 m, respectively.

Even though the proposed method based on monocular vision have some systematic errors related to image processing and tree contour extracting, it has a low and acceptable errors which fall within the accuracy requirements of Chinese national forest resources continuous inventory and can be used to survey the tree attributes [49].

V. CONCLUSION

In this paper, we present a method for tree height and crown diameter measurement based on monocular vision, and test the performance of THM and CDM. The proposed method consist of image acquisition and tree contour extraction, establishment of THM and CDM. We use Mean-Shift algorithm to segment the tree's image and extract their contours. In addition, we establish an adaptive feature coordinate system, which is the basis for constructing the measurement models. Furthermore, by analyzing the pinhole camera imaging principle, we establish a depth extraction model which is suitable for different models of smartphones and build the THM and CDM to calculate the tree's attributes from the image. The accuracy of this method falls within the requirements of Chinese national forest resources continuous inventory and provides convenient measurement for tree height and crown diameter in forest survey.

Based on the results of this study, we can conclude a new directions for feature research such as passive measurement based on monocular vision. Compared with other passive measurement methods, this study has several novelties: it does not require any calibration board and can measure more than one tree, so it is more flexible and errors caused by data fitting can be avoided. Additionally, we only need to obtain the intrinsic parameters of the smartphone camera at the first time, and then calculate the tree height and crown diameter of every tree in the image. Moreover, parameters, such as the tilted angle of tree and the slope of the ground, are introduced into the model, leading the model more applicable. However, when the tree is far away from the camera, due to the perspective transformation, the detection accuracy of its contour is reduced and the measurement accuracy of tree attributes may be affected. Therefore, in the next step of our study, we will focus on the accurate identification and detection of trees in such case. Additionally, tree height and crown diameter can be measured, unless the key points, like geometrical center

point of the tree's bottom, the tree's highest point or the crown's widest points, are obscured. Thus we will further explore and establish attributes correlation model, which can be used to estimate one attribute by giving others.

ACKNOWLEDGMENT

The authors would like to especially thank our code and field assistants: Z. Yuting, W. Xinyi, C. Xiangwu, Y. Hong, and T. Zhen.

REFERENCES

[1] R. E. Mcroberts, E. O. Tomppo, and E. Næsset, "Advances and emerging issues in national forest inventories," *Scand. J. Forest Res.*, vol. 25, no. 4, pp. 368–381, Aug. 2010, doi: 10.1080/02827581.2010.496739.

[2] J. Shi, Z. Feng, and J. Liu, "Design and experiment of high precision forest resource investigation system based on UAV remote sensing images," *Trans. Chin. Soc. Agricult. Eng.*, vol. 33, no. 11 , pp. 82–90, 2017, doi: 10.11975/j.issn.1002-6819.2017.11.011.

[3] G. Kunstler, D. Falster, D. A. Coomes, F. Hui, R. M. Kooyman, D. C. Laughlin, and L. Poorter, "Plant functional traits have globally consistent effects on competition," *Nature*, vol. 529, no. 7585, pp. 204–207, Jan. 2016, doi: 10.1038/nature16476.

[4] G. Shao, S. Zhao, and H. H. Shugart, *Forest Dynamics Modelling—Preliminary Explanations of Optimizing Management of Korean Pine Forests*. Beijing, China: Chinese Forestry Publishing House, 1996.

[5] A. Van Laar and A. Akça. *Forest Mensuration*, vol. 13. Amsterdam, The Netherlands Springer, 2007, doi: 10.1007/978-1-4020-5991-9.

[6] F. Baret, B. De Solan, R. Lopez-Lozano, K. Ma, and M. Weiss, "GAI estimates of row crops from downward looking digital photos taken perpendicular to rows at 57.5° zenith angle: Theoretical considerations based on 3D architecture models and application to wheat crops," *Agricult. Forest Meteorol.*, vol. 150, no. 11, pp. 1393–13401, 2010, doi: 10.1016/j.agrformet.2010.04.011.

[7] M. D. Avsar, "The relationships between diameter at breast height, tree height and crown diameter in Calabrian pines (Pinus brutia Ten.) of Baskonus Mountain, Kahramanmaras, Turkey," *J. Biol. Sci.*, vol. 4, no. 4, pp. 437–440, 2004, doi: 10.3923/jbs.2004.437.440.

[8] R. P. Sharma, Z. Vacek, and S. Vacek, "Modelling tree crown-to-bole diameter ratio for Norway spruce and European beech," *Silva Fenn*, vol. 51, no. 5, Art. no. 1740, 2017, doi: 10.14214/sf.1740.

[9] J. L. Araus and J. E. Cairns, "Field high-throughput phenotyping: The new crop breeding frontier," *Trends Plant Sci.*, vol. 19, no. 1, pp. 52–61, Jan. 2014, doi: 10.1016/j.tplants.2013.09.008.

[10] K. J. Puettmann, C. Messier, and D. K. Coates, *Managing Forests as Complex Adaptive Systems*. London, U.K.: The Solar Quarterly, 2013.

[11] S. Jayathunga, T. Owari, and S. Tsuyuki, "Analysis of forest structural complexity using airborne LiDAR data and aerial photography in a mixed conifer–broadleaf forest in northern Japan," *J. Forestry Res.*, vol. 29, no. 2, pp. 479–493, no. 2018, doi: 10.1007/s11676-017-0441-4.

[12] B. Stark, T. Zhao, Y. Q. Chen, "An analysis of the effect of the bidirectional reflectance distribution function on remote sensing imagery accuracy from small unmanned aircraft systems," presented at the Int. Conf. Unmanned Aircr. Syst., Arlington, VA, USA, Jun. 2016, doi: 10.1109/ICUAS.2016.7502566.

[13] A. Griebel, L. T. Bennett, D. S. Culvenor, G. J. Newnham, and S. K. Arndt, "Reliability and limitations of a novel terrestrial laser scanner for daily monitoring of forest canopy dynamics," *Remote Sens. Environ.*, vol. 166, pp. 205–213, Sep. 2015, doi: 10.1016/j.rse.2015.06.014.

[14] S. Liu, F. Baret, M. Abichou, F. Boudon, S. Thomas, K. Zhao, C. Fournier, B. Andrieu, K. Irfan, and M. Hemmerlé, "Estimating wheat green area index from ground-based LiDAR measurement using a 3D canopy structure model," *Agricult. Forest Meteorol.*, vol. 247, pp. 12–20, Dec. 2017, doi: 10.1016/j.agrformet.2017.07.007.

[15] W. Liu, T. Zhong, and Y. Song, "Prediction of trees diameter at breast height based on unmanned aerial vehicle image analysis," *Trans. Chin. Soc. Agricult. Eng.*, vol. 33, no. 21, pp. 99–104, 2017, doi: 10.11975/j.issn.1002-6819.2017.21.012.

[16] S. Xin, L. Cao, and G. She, "Subtropical forest biomass estimation based on hyperspectral and high-resolution remotely sensed data," *J. Remote Sens.*, vol. 20, no. 6, pp. 1446–1460, 2016, doi: 10.11834/jrs.20165210.

[17] S. Junling, G. Sun, P. Ma, T. Dong, and Y. Yang, "Laser target localization based on symmetric wavelet denoising and asymmetric gauss fitting," *Chin. J. Lasers*, vol. 44, no. 6, 2017, Art. no. 0604001, doi: 10.3788/CJL201744.0604001.

[18] B. Yang, F. Liang, and R. Huang, "Progress challenges and perspectives of 3D LiDAR point cloud processing," *Acta Geodaetica Et Cartograph. Sinica*, vol. 46, no. 10, pp. 1509–1516, 2017, doi: 10.11947/j.AGCS.2017.20170351.

[19] A. Ferraz, F. Bretar, S. Jacquemoud, G. Gonçalves, L. Pereira, M. Tomé, and P. Soares, "3-D mapping of a multi-layered Mediterranean forest using ALS data," *Remote Sens. Environ.*, vol. 121, pp. 210–223, Jun. 2012, doi: 10.1016/j.rse.2012.01.020.

[20] C. Liu, Y. Xing, J. Duanmu, and X. Tian, "Evaluating different methods for estimating diameter at breast height from terrestrial laser scanning," *Remote Sens.*, vol. 10, no. 4, p. 513, 2018, doi: 10.3390/rs10040513.

[21] Y. Xu, Z. Yong, X. Lu, Y. Cheng-Hua, and W. Qiang, Liu Yue-Hao, and Z. Yuan, "Increasing the range accuracy of three-dimensional ghost imaging ladar using optimum slicing number method," *Chin. Phys. B* vol. 24, no. 12, pp. 319–324, 2015, doi: 10.1088/1674-1056/24/12/124202.

[22] S. H. Ahn, J. Choi, N. L. Doh, W. K. Chung, "A practical approach for EKF-SLAM in an indoor environment: Fusing ultrasonic sensors and stereo camera," *Auton. Robots* vol. 24, no. 3, pp. 315–335, 2008, doi: 10.1007/s10514-007-9083-2.

[23] S. Kumar and H. Furuhashi, "Long-range measurement system using ultrasonic range sensor with high-power transmitter array in air," *Ultrasonics*, vol. 74, pp. 186–195, Feb. 2017, doi: 10.1016/j.ultras.2016.10.012.

[24] R. Szeliski, *Computer Vision: Algorithms and Applications*. New York, NY, USA: Springer, 2010, doi: 10.1007/978-1-84882-935-0.

[25] J. Mei, D. Zhang, and Y. Ding, "Monocular vision for pose estimation in space based on cone projection," *Opt. Eng.*, vol. 56, no. 10, Oct. 2017, Art. no. 103108, doi: 10.1117/1.OE.56.10.103108.

[26] W. Sun, L. Chen, B. Hu, L. Ren, and X. Wu, "Binocular vision-based position determination algorithm and system," presented at the Int. Conf. Comput. Distrib. Control Intell. Environ. Monit., Zhangjiajie, Hunan China, Mar. 2012, doi: 10.1109/CDCIEM.2012.47.

[27] S. Jie, L. Yinya, Q. Guoqing, and S. Andong, "Machine vision based passive tracking algorithm with intermittent observations," *J. Huazhong Univ. Sci. Technol. (Natural Sci. Ed.)*, vol. 45, no. 6, pp. 33–37, 2017, doi: 10.13245/j.hust.170607.

[28] C. Xu, D. Huang, and F. Kong, "Small UAV passive target localization approach and accuracy analysis," *Chin. J. Sci. Instrum.*, vol. 36, no. 5, pp. 1115–1122, no. 2015, doi: 10.19650/j.cnki.cjsi.2015.05.019.

[29] D. Weimin, S. Zhao, S. Zhao, J. Gu, W. Qiu, and B. Guo, "Measurement methods of fruit tree canopy volume based on machine vision," *Trans. Chin. Soc. Agricult. Machinery*, vol. 47, no. 6, pp. 1–10, 2016, doi: 10.6041/j.issn.1000-1298.2016.06.001.

[30] A. Ming, T. Wu, J. Ma, F. Sun, and Y. Zhou, "Monocular depth-ordering reasoning with occlusion edge detection and couple layers inference," *IEEE Intell. Syst.*, vol. 31, no. 2, pp. 54–65, Mar./Apr. 2016, doi: 10.1109/MIS.2015.94.

[31] E. Alexander, Q. Guo, S. Koppal, S. J. Gortler, and T. Zickler, "Focal flow: Velocity and depth from differential defocus through motion," *Int. J. Comput. Vis.*, vol. 126, no. 2, pp. 1062–1083, 2017, doi: 10.1007/s11263-017-1051-5.

[32] C. S. Royden, D. Parsons, and J. Travatello, "The effect of monocular depth cues on the detection of moving objects by moving observers," *Vis. Res.*, vol. 124, pp. 7–14, Jul. 2016, doi: 10.1016/j.visres.2016.05.002.

[33] L. Kehong, L. Jiang, and Y. Gong, "Depth map extraction methods in 2D-3D image/video conversion," *J. Image Graph.*, vol. 19, no. 10, pp. 1393–1406, 2014, doi: 10.11834/jig.20141001.

[34] H. Fathi and I. Brilakis, "Multistep explicit stereo camera calibration approach to improve euclidean accuracy of large-scale 3D reconstruction," *J. Comput. Civil Eng.*, vol. 30, no. 1, 2016, Art. no. 04014120, doi: 10.1061/(ASCE)CP.1943-5487.0000454.

[35] A.-S. Poulin-Girard, S. Thibault, and D. Laurendeau, "Influence of camera calibration conditions on the accuracy of 3D reconstruction," *Opt. Express*, 24, no. 3, pp. 2678–2686, 2016, doi: 10.1364/OE.24.002678.

[36] X. Y. Huang, F. Gao, G. Y. Xu, N. G. Ding, and L. L. Xing, "Depth information extraction of on-board monocular vision based on a single vertical target image," *J. Beijing Univ. Aeronaut. Astronaut.*, vol. 41, no. 4, pp. 649–655, 2015, doi: 10.13700/j.bh.1001-5965.2014.0272.

[37] H. Xiaodong and F. Zhongke, "Obtainment of sample tree's DBH based on digital camera," *Trans. Chin. Soc. Agricult. Machinery*, vol. 46, no. 9, pp. 266–272, 2015, doi: 10.6041/j.issn.1000-1298.2015.09.039.

[38] K. Zhou, Y. Wang, L. I. Ji, G. Jiang, and X. U. Aijun, "A study of tree measurement systems based on Android platform," *J. Nanjing Forestry Univ.*, vol. 40, no. 4, pp. 95–100, 2016, doi: 10.3969/j.issn.1000-2006.2016.04.015.
[39] G. Fangli, "The tree dbh measurement method based on smartphone and machine vision technology," Ph.D. dissertation, Zhejiang A&F Univ., Hangzhou, China, 2018.
[40] A Ferraz, F. Bretar, S. Jacquemoud, G. Gonçalves, and L. Pereira, "3D segmentation of forest structure using a mean-shift based algorithm," in *Proc. 17th IEEE Int. Conf. Image Process. (ICIP)*, Sep. 2010, pp. 1413–1416, doi: 10.1109/ICIP.2010.5651310.
[41] Z. Zhang, "A flexible new technique for camera calibration," in *Proc. IEEE Trans. Pattern Anal. Mach. Intell.*, Washington, DC, USA, Dec. 2000, p. 1330, doi: 10.1109/34.888718.
[42] Z. Zhang, "Flexible camera calibration by viewing a plane from unknown orientations," presented at the 7th IEEE Int. Conf. Comput. Vis., Corfu, Greece, Sep. 1999, doi: 10.1109/ICCV.1999.791289.
[43] X. Wu, S. Zhou, A. Xu, and B. Chen, "Passive measurement method of tree diameter at breast height using a smartphone," *Comput. Electron. Agricult.*, vol. 163, Aug. 2019, Art. no. 104875, doi: 10.1016/j.compag.2019.104875.
[44] E. Næsset, "Predicting forest stand characteristics with airborne scanning laser using a practical two-stage procedure and field data," *Remote Sens. Environ.*, vol. 80, no. 1, pp. 88–99, 2002, doi: 10.1016/S0034-4257(01)00290-5.
[45] D. Panagiotidis, A. Abdollahnejad, P. Surový, and V. Chiteculo, "Determining tree height and crown diameter from high-resolution UAV imagery," *Int. J. Remote Sens.*, vol. 38, nos. 8–10, pp. 2392–2410, 2017, doi: 10.1080/01431161.2016.1264028.
[46] A. Kato, L. M. Moskal, P. Schiess, M. E. Swanson, D. Calhoun, and W. Stuetzle, "Capturing tree crown formation through implicit surface reconstruction using airborne lidar data," *Remote Sens. Environ.*, vol. 113, no. 6, pp. 1148–1162, no. 2016, doi: 10.1016/j.rse.2009.02.010.
[47] R. Díaz-Varela, R. de la Rosa, L. León, and P. Zarco-Tejada, "High-resolution airborne UAV imagery to assess olive tree crown parameters using 3D photo reconstruction: Application in breeding trials," *Remote Sens.*, vol. 7, no. 4, pp. 4213–4232, 2015, doi: 10.3390/rs70404213.
[48] A. Paproki, X. Sirault, S. Berry, R. Furbank, and J. Fripp, "A novel mesh processing based technique for 3D plant analysis," *BMC Plant Biol.*, vol. 12, no. 1, p. 63, 2012, doi: 10.1186/1471-2229-12-63.
[49] S. Paulus, J. Behmann, A. K. Mahlein, L. Plümer, and Heiner Kuhlmann, "Low-cost 3D systems: Suitable tools for plant phenotyping," *Sensors*, vol. 14, no. 2, pp. 3001–3018, 2014, doi: 10.3390/s140203001.

WU XINMEI received the master's degree from Zhejiang Agriculture and Forestry University, Zhejiang, China. She is currently a Research Assistant with the Zhejiang Institute of Modern Agricultural Equipment Design and Research. Her main research covers machine vision and close range photogrammetry.

XU AIJUN was born in Anhui, China, in 1976. He received the Ph.D. degree in photogrammetry and remote sensing from Wuhan University, in 2007. He is currently a Professor with the School of Information Engineering, Zhejiang Agriculture and Forestry University, Hangzhou, China. His current research interests include computer application technology and the application of GIS in the direction of agricultural informatization, and so on.

YANG TINGTING was born in Anhui, China, in 1992. She received the B.S. degree in GIS from Anhui Science and Technology University, in 2017. She is currently pursuing the master's degree with Zhejiang Agriculture and Forestry University, Zhejiang, China. Her main research covers deep learning and image processing.